Supporting information

Effective generation of active hydrogen species for nitrogen fixa-tion on Pt/DUT-67(Zr)

Yun Huang [a, b], Qi Chen [a, b], Yueling Chen [a, b], Zefeng Yang [a, b], Jionghua Wu [a, c, *], Jimmy C. Yu [b, d, *], Ling Wu [a, b, *]

[a] State Key Laboratory of Chemistry for NBC Hazards Protection, College of Chemistry, Fuzhou University, Fuzhou 350116, China

[b] State Key Laboratory of Photocatalysis on Energy and Environment, College of Chemistry, Fuzhou University, Fuzhou 350116, China

[c] Institute of Micro-Nano Devices and Solar Cells, College of Physics and Information Engineering, Fuzhou University, Fuzhou 350116, China

[d] Department of Chemistry, Chinese University of Hong Kong, Shatin, New Territories, Hong Kong 999077, China

* Corresponding authors

E-mail address: JionghuaWu@fzu.edu.cn (J. Wu), jimyu@cuhk.edu.hk (J. Yu), wuling@fzu.edu.cn (L. Wu).

Table of Contents

1. Characterization

The crystal structure of the samples was analyzed on an X-ray diffractometer (ultimate IV, Rigaku) using Cu Ka radiation (λ = 0.15406 nm) in the range of 5-50. The scanning electron microscope (SEM) images of the catalysts were observed by Anfei Quantum 200 F electron microscope to clearly understand the morphology and structure of the catalysts. Transmission electron microscopy (TEM), higher-resolution transmission electron microscopy (HRTEM), and element mapping were performed using a JEOL model JEM2010 EX microscope at an accelerating voltage of 200 kV to further study the structure and elemental composition of the catalysts. X-ray photoelectron spectroscopy (XPS) results were received on a PHI Quantum 2000 XPS system with monochromatic Al Kα Radiation. The in-situ XPS spectroscopy (in-situ XPS) results were received on a Thermo ESCALAB 250Xi instrument with a 300 W Xe lamp as the light source. The UV-vis diffuse reflectance spectra (UV-vis DRS) were recorded on a UV-vis spectrophotometer (Cary 500) to reveal the optical properties of the catalysts. The FT-IR spectra were taken by a NICOLET IS50 Fourier transform infrared (FT-IR) spectrometer. The Brunauer-Emmett-Teller (BET) specific surface areas of the samples were measured on a Micrometrics ASAP 2020 M volumetric gas sorption instrument by nitrogen adsorption/desorption isotherms at 77 K. The gas chromatography (GC-7890B, Agilent) equipped with a TCD, an FID detector, and a chromatographic column (MolSieve 5A) was used to measure the amount of generated O_2. The ion chromatography instrument (SH-CIC-100) was used to measure the concentration of NH_4^+. The Steady-state photoluminescence (PL) and time-resolved PL decay spectra were measured on Fluorolog-3 type fluorescence spectrometer. (Test temperature: room temperature, light source: xenon lamp, detector: photomultiplier tube, excitation wavelength λ=360 nm). The average lifetime is calculated using the following formula: $\tau_{ave} = (A_1\tau_1^2+A_2\tau_2^2) \div (A_1\tau_1+ A_2\tau_2)$. The Bruker EPR A300 spectrometer was used to record electron paramagnetic resonance (EPR) signals and analyze the active species during the reaction.

2. Electrochemical testing

The short-circuit photocurrent response, and Nyquist impedance measurements were tested on a CHI660D electrochemical workstation, respectively. The specific experimental process is as follows: the electrochemistry tests were carried out in a conventional three-electrode cell, including the working electrode, a Pt electrode (counter electrode), and a saturated Ag/AgCl electrode (reference electrode). A clean fluorine-doped tin oxide (FTO) glass was used to prepare the working electrode. 5 mg of a sample was added into 0.5mL of dimethyl formamide and dispersed uniformly by ultrasonication. The punched tape was used to create a groove on the surface of one end of the glass. Then, 20 μL of the solution mixture was dripped into this groove. After drying, insulated nail polish was used to cover the surface of the glass except for the groove and the other end of the glass. The three electrodes and the corresponding wiring of the electrochemical workstation were connected to carry out Short-circuit photocurrent response, and Nyquist impedance measurement. The electrolytes for Nyquist impedance tests are 0.5M $K_3[Fe(CN)_6]$ and while Short-circuit photocurrent response test use 0.5M Na_2SO_4 solution, respectively.

3. Isotopic labeling experiment

Isotope labeling experiments were performed using $^{15}N_2$ (98 atoms % ^{15}N) to trace the source of ammonium obtained. For ^1H NMR measurements, the pH value of the sample solution was adjusted to 2 with hydrochloric acid and diluted with 20% DMSO-d6. The Measurements were performed on a Bruker Avance III HD 400.

4. Apparent Quantum Efficiency of Ammonia Production

Apparent quantum efficiency (AQE) was measured at ambient temperature using a 300W xenon lamp (Trustech, Beijing, PLS-SXE300c). The AQE was obtained by adding 80 mg of 5%Pt/DUT-67 to 20 mL of double deionized water in a glass reactor to irradiate an area of 4 cm^{-2}. The measured light intensity was 15.71 $mW \cdot cm^{-2}$, respectively. After 1h of photocatalytic reaction, the yield of NH_4^+ was determined, and the mole number of ammonia molecules generated was 78.8 μmol. The detailed calculation method of AQE is as follows:

$$\mathrm{AQE}(\%) = \frac{\mathrm{M} \times \mathrm{N_A} \times \mathrm{N_e}}{\frac{\mathrm{P} \times \mathrm{A} \times \mathrm{t}}{\mathrm{h} \times \mathrm{v}}} \times 100\%,$$

Where M represents the molar number of generated ammonia molecules during the irradiation time t, and P, and A, are the incident light intensity, light incident area, and frequency, respectively; N_A and h are the Avogadro's constant and Planck constant, respectively.

The calculation formula of AQE is as follows:

$$\begin{aligned}
\mathrm{AQE}(\%) &= \frac{\mathrm{N_{reacted}}}{\mathrm{N_{incident}}} \times 100\% \\
&= \frac{\mathrm{M} \times \mathrm{N_A} \times \mathrm{N_e}}{\frac{\mathrm{P} \times \mathrm{A} \times \mathrm{t}}{\mathrm{h} \times \mathrm{v}}} \times 100\% \\
&= \frac{\mathrm{M} \times \mathrm{N_A} \times \mathrm{N_e}}{\frac{\mathrm{P} \times \mathrm{A} \times \mathrm{t} \times \lambda}{\mathrm{h} \times \mathrm{c}}} \times 100\% \\
&= \frac{157.6\ \mu\mathrm{mol} \times 6.02 \times 10^{23}\mathrm{mol}^{-1} \times 0.61 \times 3}{\frac{15.71\ \mathrm{mW{\cdot}cm^{-2}} \times 4\ \mathrm{cm^2} \times 3600\ \mathrm{s} \times 280\ \mathrm{nm}}{6.63 \times 10^{-34}\ \mathrm{Js} \times 3 \times 10^{8}\ \mathrm{ms^{-1}d}}} \times 100\% \\
&= 1.37\%
\end{aligned}$$

5. Computational details

The density functional theory (DFT) calculations were performed by employing the universal generalized gradient correlation function and Vienna ab initio simulation package (VASP5.4). A plane-wave basis set with a cutoff energy at 400 eV within the framework of the projector augmented wave method was adopted. The Gaussian smearing width was set to 0.2 eV. The Brillouin zone was sampled with a 3 × 3 × 1 K points. All atoms were allowed to converge to 0.01 eV $Å^{-1}$. The adsorption energy of N_2 molecule on catalyst is defined as:

$E = E_{tot} - E_{cat} - E_{N_2}$

where E_{tot}, E_{cat} and E_{N_2} demonstrate the total energies of catalyst with N_2 adsorption, catalyst before N_2 adsorption, and isolated N_2 molecule.

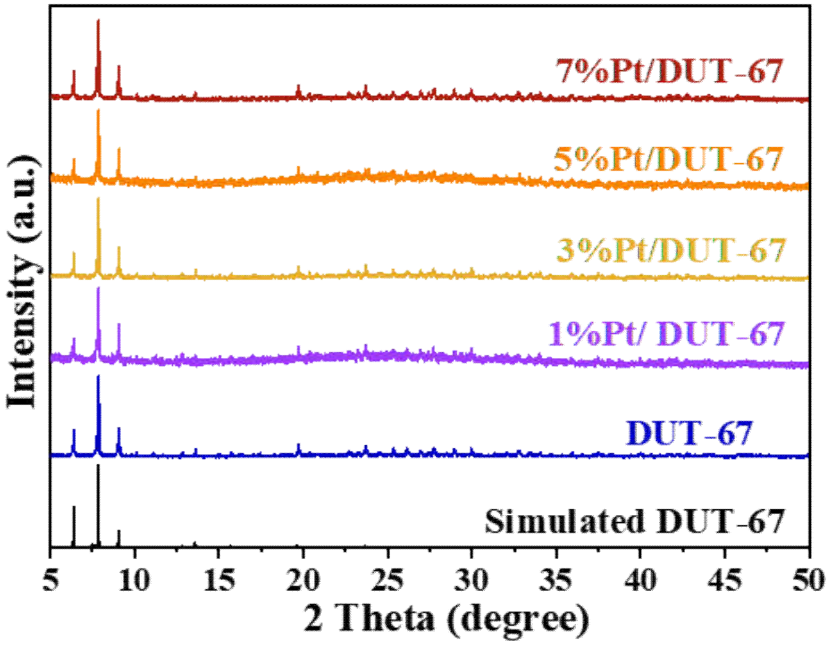

Fig. S1 XRD patterns of DUT-67 and Pt/DUT-67.

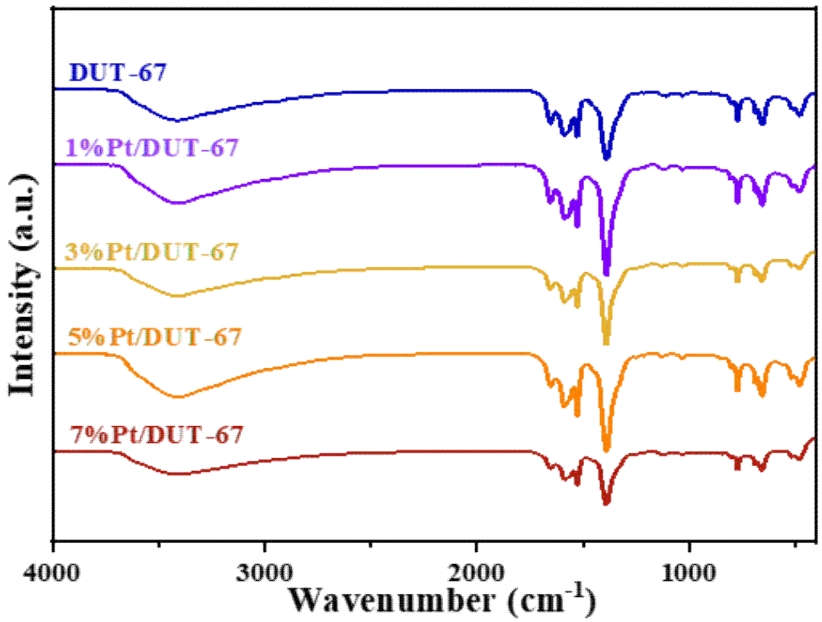

Fig. S2 FT-IR spectra of DUT-67 and Pt/DUT-67.

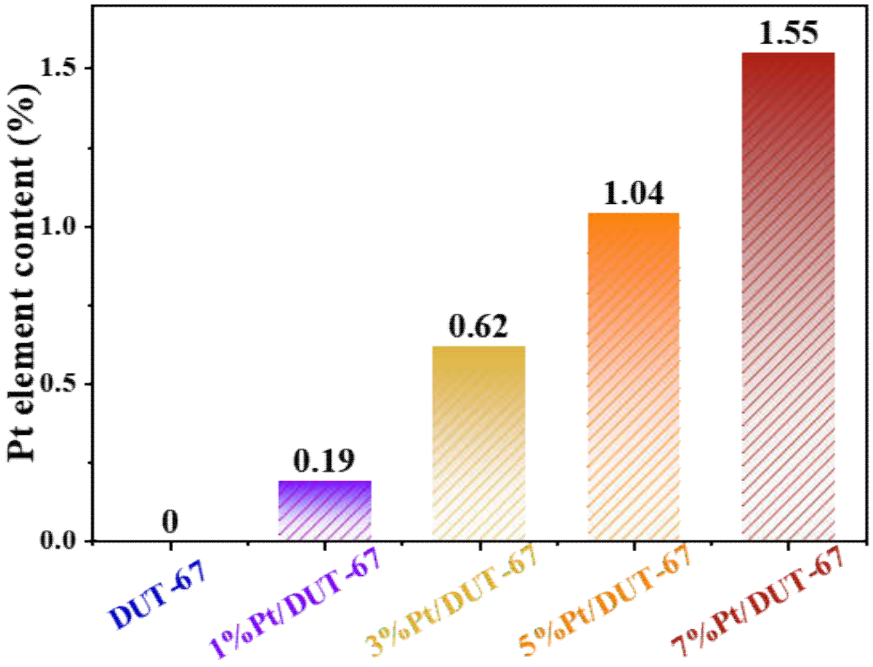

Fig. S3 Actual weight percentage of Pt element in Pt/DUT-67.

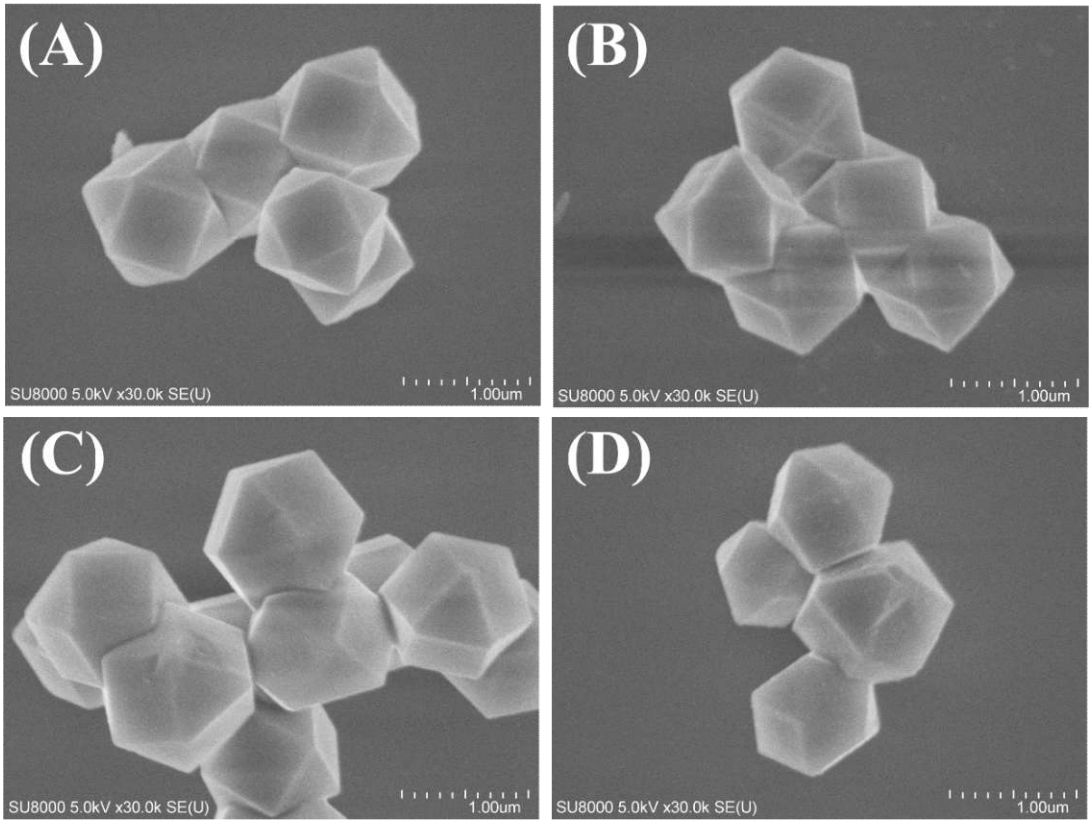

Fig. S4 SEM images of (A) DUT-67, (B) 1%Pt/DUT-67, (C) 3%Pt/DUT-67, and (D) 7%Pt/DUT-67.

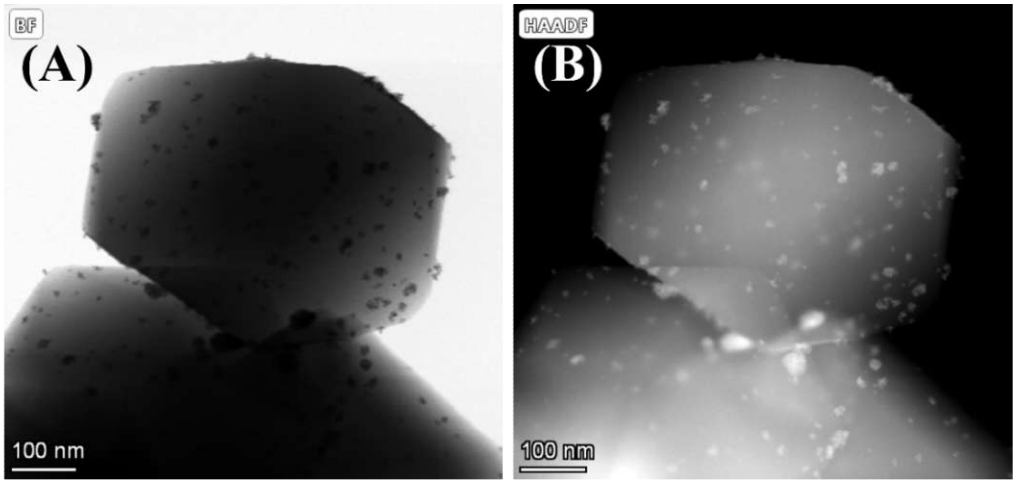

Fig. S5 SEM image of (A) bright and (B) dark fields of 5%Pt/DUT-67.

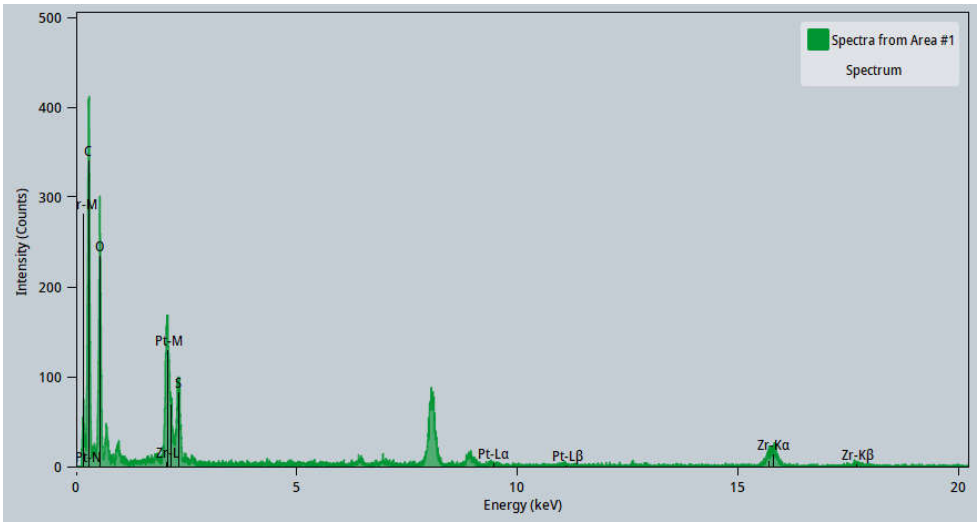

Fig. S6 EDS image.

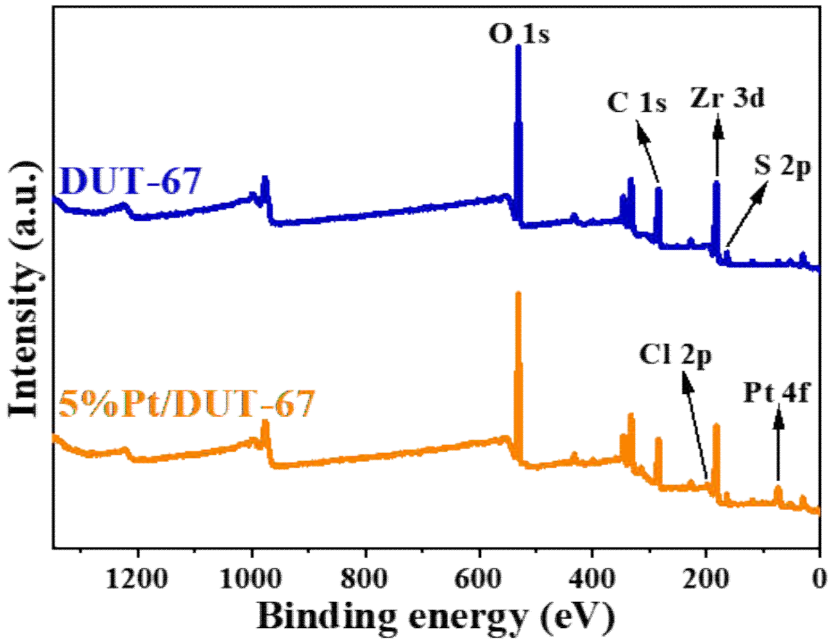

Fig. S7 XPS survey spectra of DUT-67 and 5%Pt/DUT-67.

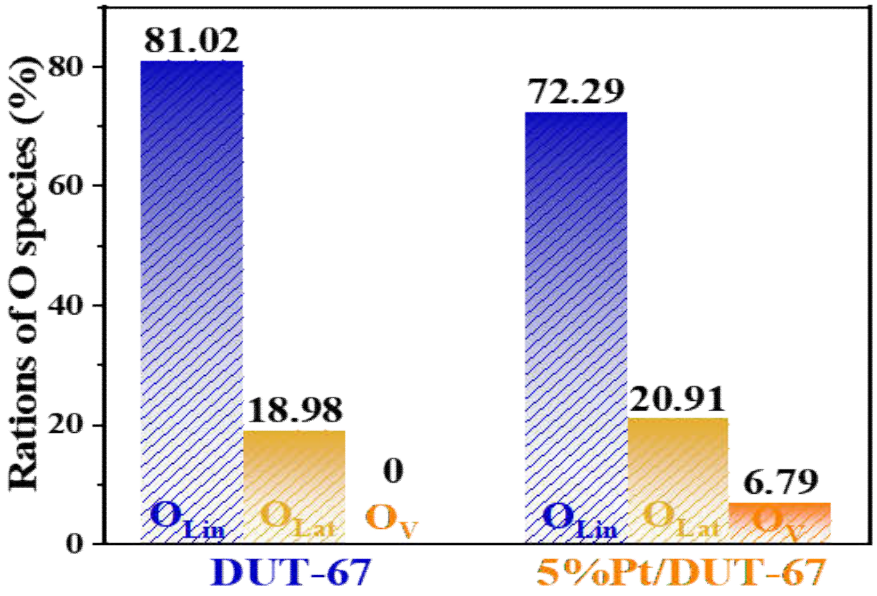

Fig. S8 Proportion chart of O species.

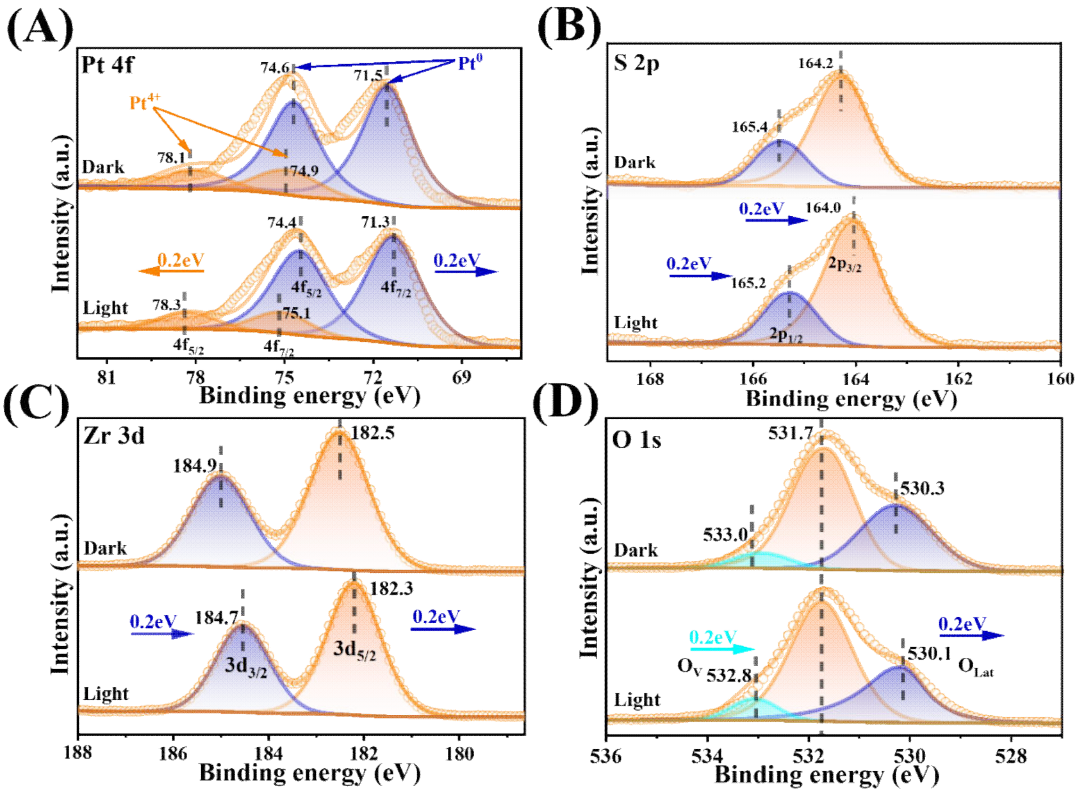

Fig. S9 (A) Pt 4*f* XPS spectra, (B) S 2*p* XPS spectra, (C)Zr 3*d* XPS spectra, (D)O 1*s* XPS spectra of in situ XPS measurements for 5%Pt/DUT-67 with or without light. states.

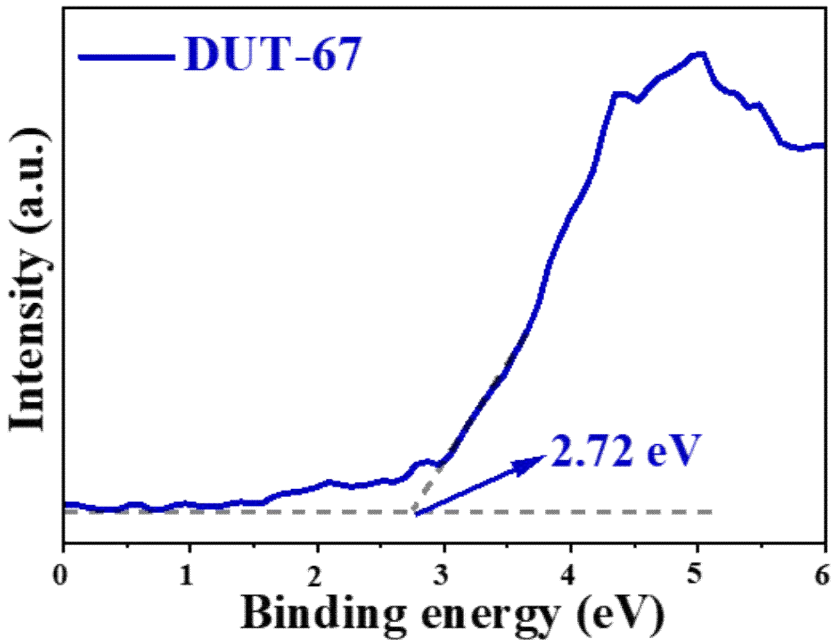

Fig. S10 Valence Band XPS Spectrum of DUT-67.

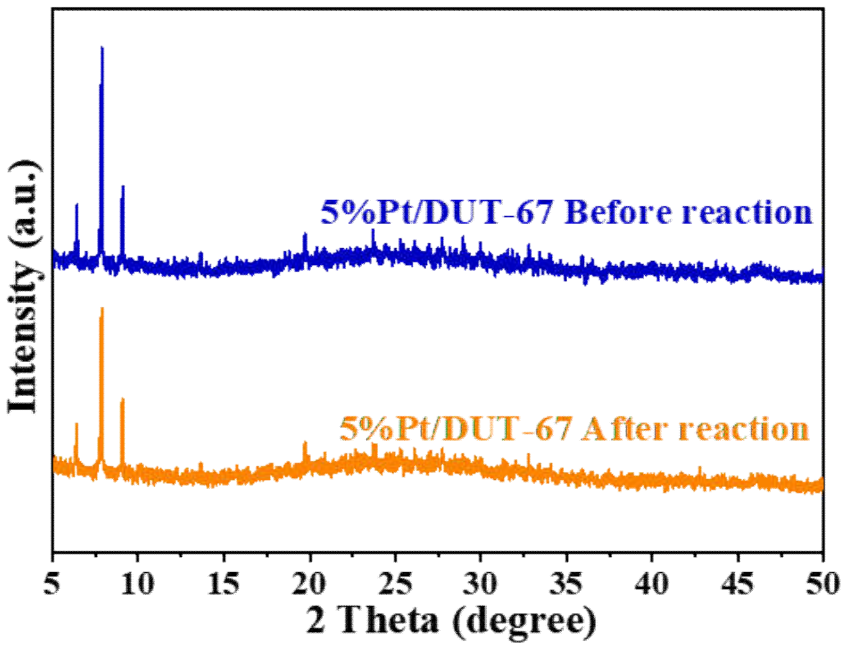

Fig. S11 XRD patterns of 5%Pt/DUT-67 before and after reaction.

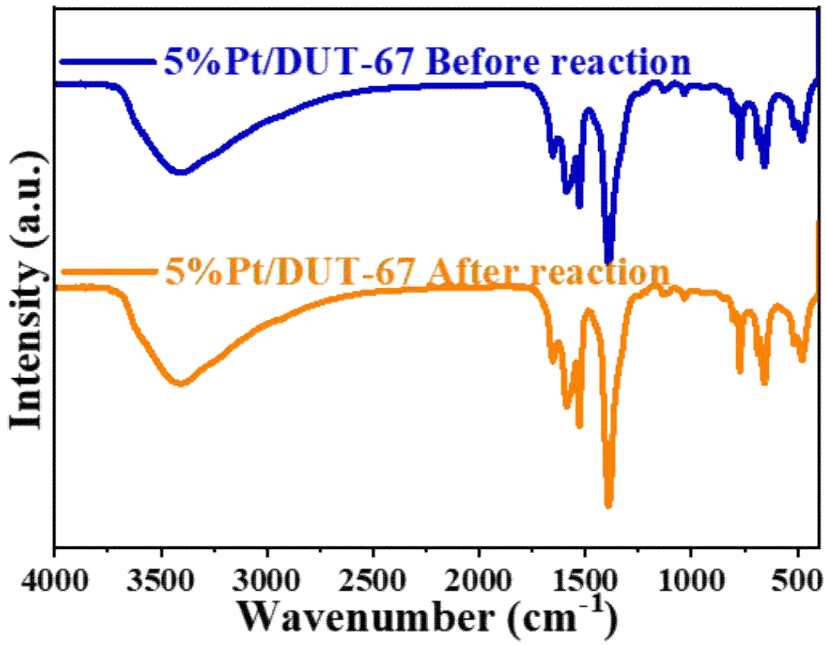

Fig. S12 FT-IR spectra of 5%Pt/DUT-67 before and after reaction.

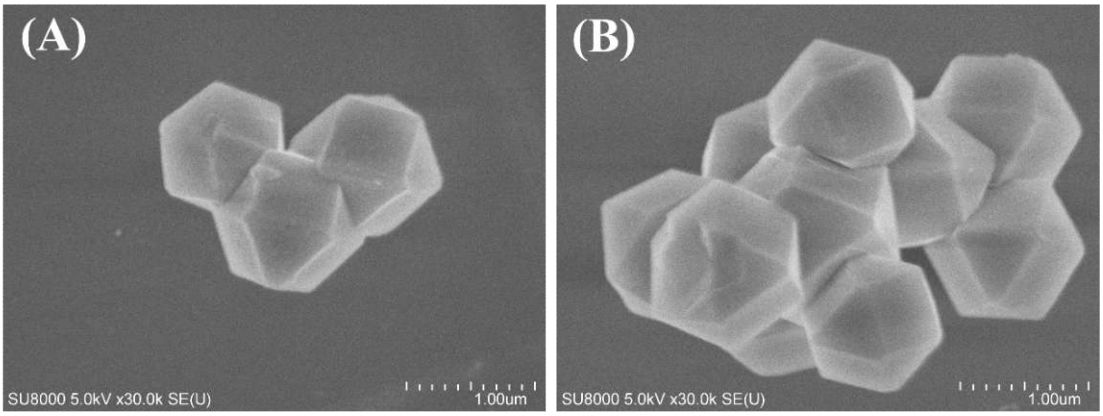

Fig. S13 SEM images of 5%Pt/DUT-67 (A) before and (B) after reaction.

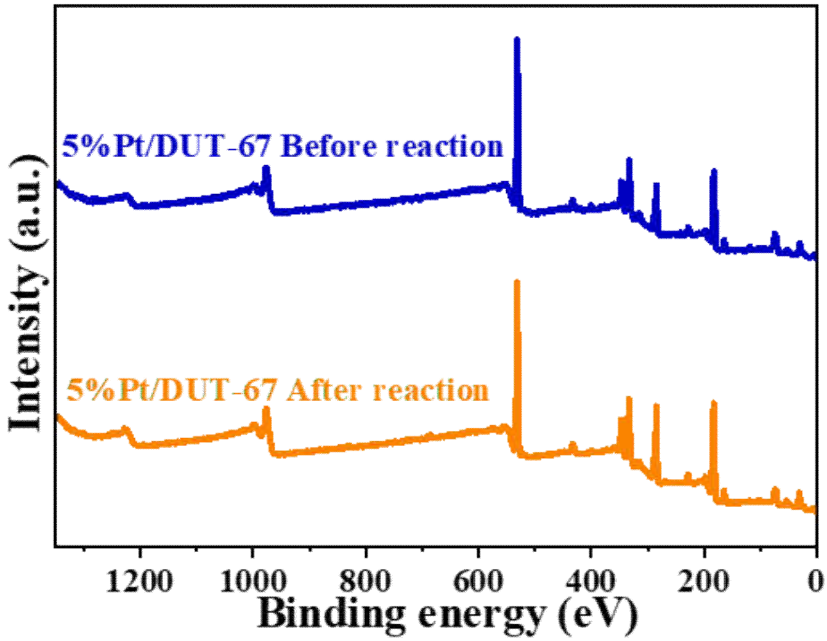

Fig. S14 XPS survey spectra of 5%Pt/DUT-67 before and after reaction.

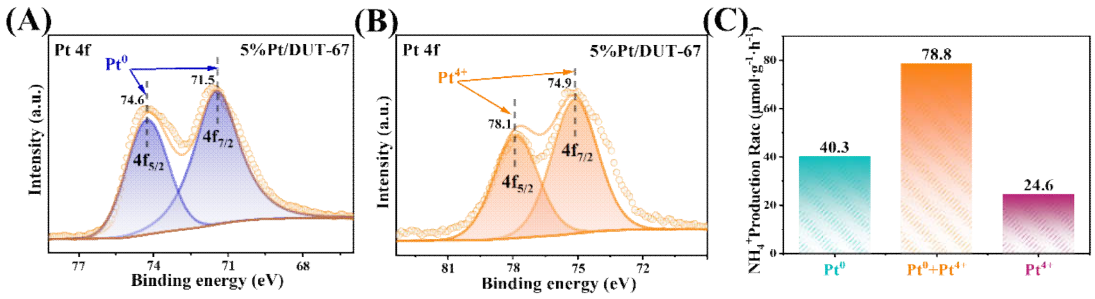

Fig. S15 (A) (B) XPS survey spectra of 5%Pt/DUT-67 Pt 4*f*. (C) Photocatalytic nitrogen fixation performance of clustered (Pt^0) and single-atom (Pt^{4+}) states.

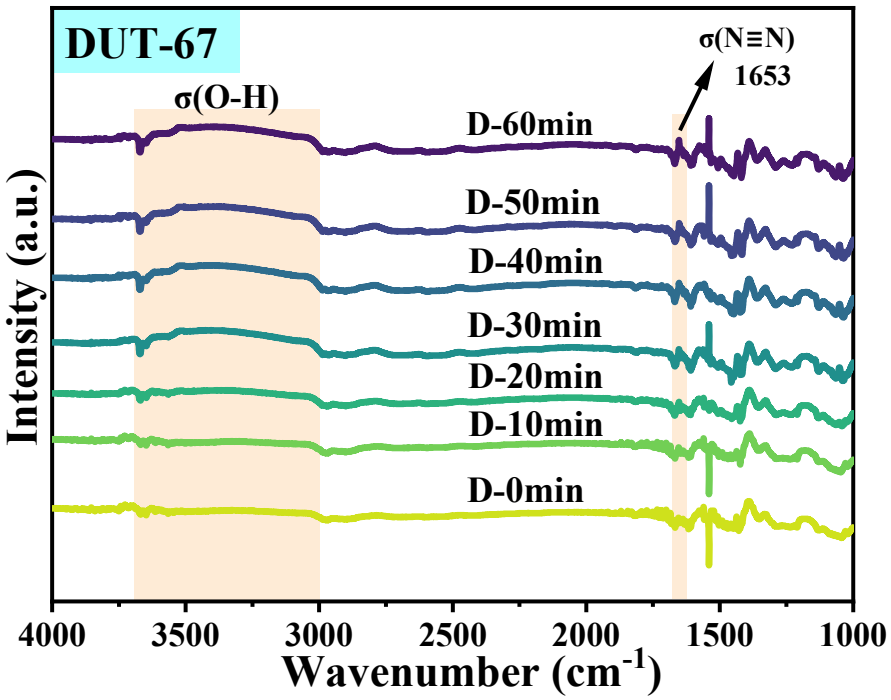

Fig. S16 In situ DRIFTS of DUT-67 in N_2 atmosphere under dark condition.

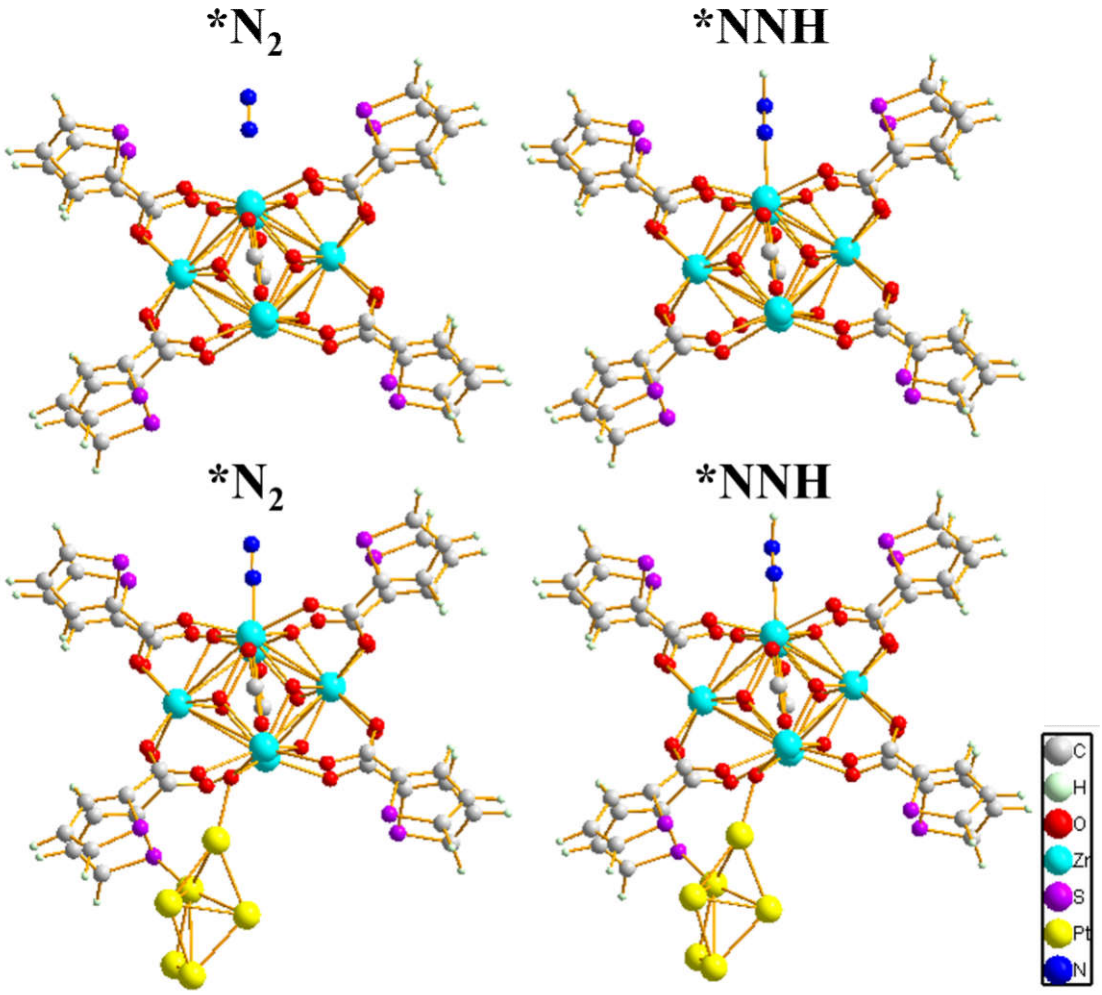

Fig. S17 Schematic of the nitrogen activation and nitrogen hydrogenation processes for DUT-67 and Pt/DUT-67.

Sample	Actual Pt (wt%)
DUT-67(Zr)	0.00
1%Pt/DUT-67	0.19
3%Pt/DUT-67	0.62
5%Pt/DUT-67	1.04
7%Pt/DUT-67	1.55

Table S1. The actual content of Pt in the prepared samples characterized by ICP-OES.

Sample (5%Pt/DUT-67)	Actual Pt (wt%)
before reaction	1.04
after reaction	1.02

Table S2. The actual content of Pt of 5%Pt/DUT-67 before and after reaction characterized by ICP-OES.